

# Learning Probabilistic Awareness Models for Detecting Abnormalities in Vehicle Motions

Damian Campo<sup>ID</sup>, Mohamad Baydoun, Pablo Marin<sup>ID</sup>, David Martin,  
Lucio Marcenaro, Arturo de la Escalera, and Carlo Regazzoni

**Abstract**—This paper proposes a method to detect abnormal motions in real vehicle situations based on trajectory data. Our approach uses a Gaussian process (GP) regression that facilitates to approximate expected vehicle's movements over a whole environment based on sparse observed data. The main contribution of this paper consists in decomposing the GP regression into spatial zones, where quasi-constant velocity models are valid. Such obtained models are employed to build a set of Kalman filters that encode observed vehicle's dynamics. This paper shows how proposed filters enable the online identification of abnormal motions. Detected abnormalities can be modeled and learned incrementally, automatically by intelligent systems. The proposed methodology is tested on real data produced by a vehicle that interacts with pedestrians in a closed environment. Automatic detection of abnormal motions benefits the traffic scene understanding and facilitates to close the gap between human driving and autonomous vehicle awareness.

**Index Terms**—Smart mobility, self-aware systems, intelligent systems, trajectory modeling, decision systems.

## I. INTRODUCTION

MONITORING systems that understand observed agents' dynamics are essential for providing security and improving autonomous decision-making processes [1], [2]. Semi-autonomous systems have become a hot research field due to their potentiality at describing contextual information and detecting abnormalities automatically by using sensory data [3], [4]. In transportation, more and more proactive semi-autonomous systems are used to path planning and monitoring

Manuscript received July 24, 2018; revised December 21, 2018; accepted March 11, 2019. This work was supported in part by the Italian Ministry of University and Research for the National Technological Cluster for the Smart Communities through the Mobilità Intelligente Ecosostenibile (MIE) Project and in part by the Education, Audiovisual and Culture Executive Agency (EACEA) through the Program of Erasmus Mundus Joint Doctorate in Interactive and Cognitive Environments (EMJD ICE). The work of C. Regazzoni was supported by the UC3M-Santander Chairs of Excellence Program. The Associate Editor for this paper was P. Ye. (*Corresponding author: Damian Campo.*)

D. Campo, M. Baydoun, and L. Marcenaro are with the Department of Electrical, Electronics and Telecommunication Engineering and Naval Architecture, University of Genoa, 16145 Genoa, Italy (e-mail: damian.campo@ginevra.dibe.unige.it; mohamad.baydoun@ginevra.dibe.unige.it; lucio.marcenaro@unige.it).

P. Marin, D. Martin, and A. de la Escalera are with the Intelligent Systems Laboratory, Department of Systems Engineering and Automation, Universidad Carlos III de Madrid, 28911 Leganés, Spain (e-mail: pamarinp@ing.uc3m.es; dmgomez@ing.uc3m.es; escalera@ing.uc3m.es).

C. Regazzoni was with the Intelligent Systems Laboratory, Department of Systems Engineering and Automation, Universidad Carlos III de Madrid, 28911 Leganés, Spain. He is now with the Department of Electrical, Electronics and Telecommunication Engineering and Naval Architecture, University of Genoa, 16145 Genoa, Italy (e-mail: carlo.regazzoni@unige.it).

Digital Object Identifier 10.1109/TITS.2019.2909980

environments [5], demonstrating that such systems contribute effectively to the surveillance and exploration of environments.

Nowadays, methods based on machine learning techniques together with signal processing procedures are employed by researchers to build models that facilitate the inference of future states. Novel methods for representing data and estimating future events are used in areas such as activity/motion recognition [6], security/prevention of incidents [7] and travel management in cities and urban planning/design [2], [8].

Location of moving agents has been used by intelligent systems to generate models and perform decision-making processes. Such systems can predict future trajectory states and classify observed situations into a set of events [17]–[19]. These types of approaches that aim at analyzing agents' location data can be employed to improve transportation systems.

Fields such as: (i) traffic congestion and vehicle management [9]–[11], (ii) transit oriented development [12], [13] and (iii) smart mobility/transportation [14]–[16] can benefit significantly from inference models capable of detecting abnormalities in an online way and modifying their estimation models incrementally based on new observed experiences.

In transportation systems, researchers are interested in vehicles capable of identifying new situations and generate models that explain them on the fly, i.e., as observations are acquired [20]. Such online learning process can be achieved by allowing machines to anticipate future situations and incorporate new knowledge about observed experiences into their models. A high impact on transport policy analysis and traffic decision-making could be accomplished through this kind of reasoning.

Recent approaches proposed by [21], [22] present solutions for optimizing the transportation accessibility, i.e., the ability for moving agents to accomplish desired activities, destinations; and services by considering a transit network among involved agents. These works are based inherently on modeling trajectories as interactions between observed agents and their surroundings.

Our method considers a probabilistic approach to represent dynamic relationships among moving agents and their surroundings. Such representation enables to make future inferences of agents' states as proposed in [23], [24].

This work proposes a method where trajectory data from a moving agent is initially defined as normal. A set of discrete components codifies normal motions employed for predicting future events. As trajectories are obtained, our system evaluates their level of abnormality according to the current system's knowledge. Proposed anomaly measurements can be

useful to detect non-stationary conditions where trajectory data does not follow previously learned behaviors.

When available models do not describe observed dynamics accurately, new models have to be learned by the autonomous system. Such process facilitates the incremental learning of models that describe the normality in the scene.

This paper proposes a methodology based on the application and discretization of a Gaussian Process (GP) regression that relates vehicles' positions in an environment, i.e., spatial coordinates, with their motions, i.e., displacements. Innovations from a set of Kalman filters (KFs) are employed to determine irregularities in vehicles' dynamics inside an environment. In this work, the online detection of abnormalities related to vehicle-pedestrian interactions is considered as a proof of concept that shows the possibility of recognizing previously unseen vehicles' maneuvers that can be helpful for surveillance, decision-making, and automation in intelligent transportation contexts.

The novelties of this paper are listed as follows:

(i) The use of a GP regression that facilitates to map relationships between agents' positions and their motions. Accordingly, it is obtained the most probable agents' motion depending on where they are.

(ii) A segmentation of agents' state space from GP results, which facilitates the generation of spatial zones with high certainty (low variance) where quasi-constant velocity models are valid. Such segmentation is based on a Superpixel-like algorithm that facilitates the obtainment of space areas where normal KF models are accurate. The proposed methodology considers an incremental approach, such that new (abnormal) experiences can be added as part of inference models and employed for future inferences.

(iii) A set of filters which encode the most probable agents' motions based on past experiences. Such filters are used for making predictions of future agents' dynamics. Deviations from such predicting phase are employed for detecting abnormalities in an online quantitative way. Resulting anomaly patterns are related to previously unseen motion maneuvers.

Since the proposed methodology aims at the dynamical representation of motions generated by moving agents, our approach can be potentially used to recognize and characterize traffic situations in urban and road environments.

A practical limit of the proposed approach should be considered when the state space dimensionality is high. Nonetheless, for low dimensions of the state space, i.e., up to 3-dimensional coordinates, the proposed approach produces interesting results at modeling trajectories. For evaluation purposes, a standard vehicle task is first defined and characterized. Then, it is introduced some abnormal scenarios where the vehicle reacts to pedestrians in the scene and returns to its normal path. Results suggest that abnormalities can be detected and potentially included as part of the surveillance knowledge in an online fashion.

The rest of this paper is divided in the following way: Section II shows similar works that have tackled the problem of abnormality detection based on information related to moving agents. Section III presents some background necessary to understand the proposed methodology. Section IV explains our

proposal for modeling and incrementally recognizing motion abnormalities. Section V describes the dataset on which our algorithms are tested. Finally, the obtained results are depicted in VI and some conclusions are mentioned in VII.

## II. RELATED WORKS

Many surveillance applications require analyzing observed moving agents' motions to understand the normal/abnormal dynamics inside a scene. Through such analysis, autonomous systems can detect dangerous situations [25], [26]. Abnormality detection leads to a traffic scene understanding that facilitates the automatic modeling and analysis of trajectory data [27]. Anomaly detection strategies have been applied to several transportation-related domains, such as crowded scenes [28], traffic monitoring [29], robot mobility [30], maritime transportation [31], among others. In such works, normality is defined by a set of observed organized behaviors. Hence, abnormalities are activities that do not match with patterns previously learned as normal. In other words, anomalies are behaviors that have not been observed before [32].

Nowadays, trajectories of vehicles offer a vast variety of information that can be analyzed to train intelligent systems that understand the vehicles' surroundings [33]. Such systems create new self-aware capabilities in autonomous driving systems that could be beneficial in real traffic scenarios. In this work, self-awareness is understood as the system's ability to interpret measurements, detect abnormal observations and adapt to unseen situations. Accordingly, self-aware autonomous driving capabilities include the understanding of trajectory maneuvers, recognition of trajectory patterns and decision-making processes. Recent autonomous vehicles can react, make decisions and change their behaviors in response to sensory information of their surroundings [34], [35]. A system with awareness capabilities allows vehicles to actively identify, differentiate and classify states to determine next actions autonomously. The work presented in [36] analyzes an algorithm that allows an autonomous system to determine the optimal sequences of actions to avoid obstacles while wandering dynamically around a changing environment without prior knowledge about its surroundings. The work in [37] presents a robot's learning mechanism that adjusts the sensorimotor mapping at every learning step, helping the robot to choose motions. Such a robot is endowed with the abilities of self-learning and self-assessment so that it can learn the skills to keep itself balance while interacting with the environment.

In [38], a hidden Markov model (HMM) is applied to represent normal activities and perform anomaly detection. This work evidences how trajectory modeling can be useful for detecting unusual movements in video sequences. Additionally, works proposed by [25] and [39] show the possibility of learning dynamic models based on spatial trajectory observations and demonstrate how sparse information of agents' motions can be used for detecting abnormal behaviors.

Existing approaches based on trajectory modeling can be categorized into two main branches [38]. (i) *Similarity-based approaches*: which define pairwise similarities between trajectories processed by some clustering algorithm according to some measures [40]. (ii) *Motion-based approaches*: where

a mapping of input trajectories is described by combining the dynamics of all moving agents over time. This paper proposes a fusion of both methodologies since it is performed an extraction of semantic regions based on simple dynamic models. A GP regression methodology is employed to model trajectories and regularize data. Also, a clustering algorithm based on an over-segmented (OS) Superpixel approach is considered for identifying relevant dynamical zones that facilitate the reduction of dimensionality and the detection of abnormalities.

The present paper proposes an abnormality detection method to be applied in traffic scenes where location data from vehicles is available. In such kind of scenarios, measured location data usually covers a specific portion of the whole observable environment. Our work employs a GP regression that uses measured evidence for making an approximation of the most probable motions over the entire traffic environment. The GP application facilitates the generalization of effects related to an activity/situation through the whole spatial plane by using a probabilistic framework. GP's outputs are employed to recognize important zones where basic models are valid. Recognized areas are then used for building a set of filters employed for abnormality recognition purposes.

Recently, [19] has introduced a methodology for modeling and classifying location data. Such a methodology uses a GP technique [32] coupled with a Superpixel algorithm [41] for identifying areas characterized by simple dynamic models. The effort presented in [19] motivates our work significantly. However, this paper differs from [19] in that: (i) Instead of modeling the angle (direction) and speed (velocities' magnitude); agents' displacements are modeled directly in the environment's coordinate system. (ii) This work codifies GP outputs under an OS hypothesis which offers a more precise clustering process. By considering such reasoning, it is possible to recognize more accurately the regions (zones) where linear dynamic models are valid. (iii) This work proposes a measurement for abnormality detection based on innovations produced by a set of KFs that encode the normal (expected) situations. (iv) Proposed techniques are evaluated in real data of a vehicle moving in a closed environment. Interactions between vehicle and pedestrians are analyzed and detected as abnormalities.

The proposed method contributes to the state of the art since: (i) It enables to model uncertainties at different levels of inference which leads to a more accurate detection of abnormalities. (ii) It is a general formulation that could work several types of state information (not necessarily position data). (iii) It facilitates not only to detect anomalies but offers the possibility to easily learn and use them through KF models.

### III. MATHEMATICAL BACKGROUND

The proposed approach models agents' state spaces dynamically under a probabilistic framework. Our method uses Bayesian reasoning for interpreting and model observed data. Agents' states are organized in such a way that a GP regression can be applied to understand their dynamics depending on their location in the environment. This section focuses on

the technicalities associated with the Bayesian representation of trajectory data and the theory behind the nonparametric learning of state relationships made by the GP regression.

#### A. Bayesian Modeling of Spatial Trajectories

Let  $x \in \mathbb{R}^d$  be a generalized coordinated system, such that the scene is described by a  $d$ -dimensional space. The state of a given moving agent ( $l$ ) is defined as a vector composed of its positions and  $m$  time derivatives, such that  $X_{(l)} = [x_{(l)} \dot{x}_{(l)} \cdots x_{(l)}^{(m)}]^T$ .

This work considers temporal dependencies for each moving agent's dynamics of the type  $p(X_{(l),k}|X_{(l),k-1})$ , i.e., current states depend on the past information. Where  $X_{(l),k} = [x_{(l),k} \dot{x}_{(l),k} \cdots x_{(l),k}^{(m)}]^T$  represents the state of an agent ( $l$ ) at a particular time instant  $k$ .

For modeling the evolution of states through time. It is proposed a dynamic model that relates present and future states. Consequently, it is introduced a dynamic equation that describes the agents' state transition model, such that:

$$X_{(l),k} = f_A(X_{(l),k-1}) + w_k, \quad (1)$$

where  $w_k$  represents the process noise introduced by the function  $f_A(\cdot)$ .  $A$  encodes the way by which an agent moves when it is affected by a certain motivation. In that sense,  $A$  indexes the identified organized motions produced by an external entity. Such variable follows the reasoning of static motivation spots described previously in [26].

Since measurements from devices are employed to infer agents' states, an observation model can be defined as:

$$Z_{(l),k} = h(X_{(l),k}) + v_k, \quad (2)$$

where  $Z_k$  is the agent's observation at the time instant  $k$ ,  $v_k$  is the observation noise introduced by the measurement device.  $h(\cdot)$  is a function that maps agents' states into observations.

Our method uses a Dynamical Bayesian network (DBN) for representing and modeling situations where location measurements  $Z$  are available. DBNs are suitable for describing agents' dynamics due to their capability of modeling future instances based on observations in a probabilistic way. Such a characteristic is useful when performing tracking and recognizing abnormalities in transportation scenarios [27], [42].

#### B. Gaussian Process Regression

A GP is a statistical model where observations occur in a continuous domain, e.g., locations, velocities or time. GPs associate a normal distributed random variable to points in a continuous space. A GP can be seen as the probability distribution over the function:

$$g(\mathcal{X}) \sim GP(\mu(\mathcal{X}), \Sigma(\mathcal{X})), \quad (3)$$

where,  $g(\cdot)$  is distributed as a GP with mean function  $\mu(\mathcal{X})$  and covariance function  $\Sigma(\mathcal{X})$ .

GPs are widely used as prior functions in nonlinear-nonparametric regressions and classification problems. The goal of GP regressions is to find a function  $g(\cdot)$  that relates input  $\mathcal{X}$  with output  $\mathcal{Y}$  data, such that:

$$\mathcal{Y} = g(\mathcal{X}) + \epsilon, \quad (4)$$

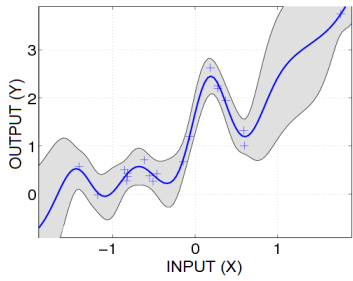


Fig. 1. 1-dimensional GP regression example, taken from [43].

TABLE I  
MATHEMATICAL NOTATIONS

$Z_{(l),k}$	$\triangleq$	Location measurement of the agent at a time $k$
$X_{(l),k}$	$\triangleq$	State of agent $l$ measurement at a time $k$
$U_{(l),k}$	$\triangleq$	Velocity of agent $l$ at a time $k$
$\hat{Y}_{(l),k}^{(0)}$	$\triangleq$	Non-motivated model's innovation for agent $l$ at a time $k$
$\hat{X}_{k k-1}^{(0)}$	$\triangleq$	State prediction from a non-motivated model
$\hat{X}_{k k-1}^{(1)}$	$\triangleq$	State prediction from a motivated model
$\mathfrak{X}_A$	$\triangleq$	GP's location grid for an activity $A$
$\mathfrak{V}_A$	$\triangleq$	GP's innovation (velocity) grid for an activity $A$
$\mathfrak{U}_A$	$\triangleq$	GP's uncertainty grid for an activity $A$
$\xi_{A,q}$	$\triangleq$	GP's joint uncertainty grid for an activity $A$
$\lambda_{val}$	$\triangleq$	Threshold to identify valid GP's information
$\mathfrak{C}_{\mathcal{X},n}^A$	$\triangleq$	Grid location information related to over-segmented region $n$ for an activity $A$
$\mathfrak{C}_{\mathcal{Y},n}^A$	$\triangleq$	Grid innovation (velocity) information related to over-segmented region $n$ for an activity $A$
$\lambda_{bhat}$	$\triangleq$	Threshold for merging over-segmented regions
$n_k$	$\triangleq$	Grown region activated at time $k$
$A_k$	$\triangleq$	Activity executed at time $k$

where  $\epsilon$  represents the estimation error.  $g(\cdot)$  is a function that relates input and output data. Fig. 1 shows a simple example of a GP regression between one-dimensional input and output variables. Blue crosses in Fig. 1 indicate the observed information whereas the blue line represents the non-parametric function  $g(\cdot)$ . The gray contour captures the uncertainty of GP's estimations. Note that gray areas become wider (more uncertain), in cases where no evidence (absence of observations) is available, indicating that estimations in such points are less reliable.

#### IV. METHOD

This section explains the proposed approach for detecting abnormalities by using location data of moving agents. It introduces a method for decomposing GP data into zones where linear models are valid. It explains also how such models can be employed by a DBN architecture for tracking new agents and detecting anomalies. Table I lists the mathematical notations of the most relevant variables used our method.

##### A. Building of Dynamical Models

Starting from observations of agents' positions, this step enables to obtain linear models that describe the dynamics of observed agents. Our method uses a simple baseline model

from which more complex dynamics are learned. Such a baseline model assumes that agents move arbitrarily around their locations due to the lack of a motivator of action [44].

1) *Non-Motivated Dynamical Model*: Let agents' states be composed of their position and velocity, such that:  $X_{(l),k} = [\mathbf{x}_{(l),k}, \dot{\mathbf{x}}_{(l),k}]^T$ , where  $k$  indexes a given time instant and  $(l)$  labels a particular moving agent. A non-motivated dynamical model based on a random walk model is written as follows:

$$X_{(l),k+1} = F X_{(l),k} + w_{(l),k},$$

where  $w_{(l),k}$  is assumed to be drawn from a zero mean multivariate normal distribution with covariance  $Q_{(l),k}$ , such that  $w_{(l),k} \sim \mathcal{N}(0, Q_{(l),k})$ .  $F$  can be written as:

$$F = \begin{bmatrix} I_d & 0_{d,d} \\ 0_{d,d} & 0_{d,d} \end{bmatrix}, \quad (5)$$

where  $d$  represents the number of dimensions of the environment space  $\mathbf{x}$ .  $I_n$  represents the  $n \times n$  identity matrix and  $0_{n,n}$  a  $n \times n$  square zero matrix.

As can be seen from equation (5), the non-motivated model suggests that agents will rest in a quasi-static location and only random noise perturbations, modeled by  $w_{(l),k}$  will affect their states. Such assumption implies that covariance components  $Q_{(l),k}$  are small enough to model subtle random effects that an agent with no motivations can have, i.e., random oscillations around a given point. Additionally, assuming that only observations of agents' locations,  $Z$ , are available, it is possible to write:

$$Z_{(l),k} = H X_{(l),k} + v_{(l),k}, \quad (6)$$

where  $v_{(l),k} \sim \mathcal{N}(0, R_{(l),k})$ .  $R_{(l),k}$  represents the measurement covariance noise.  $Z_k$  is the individual's measured position at the time  $k$ . The matrix  $H$  has the following form:

$$H = [I_d \ 0_{d,d}].$$

2) *Motivated Dynamical Model*: A control input term,  $U$ , is introduced into equation (5) for modeling motivators' effects acting on agents in particular environment's locations. The following equation describes motivated dynamical models:

$$X_{(l),k+1} = F X_{(l),k} + B U_{(l),k} + w_{(l),k}, \quad (7)$$

where

$$B = \begin{bmatrix} \Delta k I_d \\ I_d \end{bmatrix},$$

the parameter  $U_k$  is a velocity component that encodes the effect of surroundings.  $U_k$  consists of the summed influence from diverse motivations that affect a given agent, such that:

$$U_{(l),k} = \sum_{m=1}^M u_k^{(m)}, \quad (8)$$

where  $u_k^{(m)}$  represents the motion effect produced by a motivation  $m$ .  $M$  is the total number of motivators acting on agent  $l$ . Velocity components  $U_{(l),k}$  in equation (7) are function of the agent's position  $H X_{(l),k}$ , which leads to:

$$U_{(l),k} \equiv U(H X_{(l),k}). \quad (9)$$

For agents belonging to the same class, i.e., objects with similar motion capabilities, effects acting on them are assumed to be identical for all agents, so that  $X_k = X_{(l),k}$ .

For approximating the values of  $U_k^{(l)}$ , it is considered the innovation components produced by a non-motivated model. Such innovations are defined as:

$$\tilde{Y}_k^{(0)} = Z_k - H \hat{X}_{k|k-1}^{(0)}, \quad (10)$$

where the parameter **(0)** indexes estimations made by a model based on the non-motivated dynamical behavior, see equation (5).  $\hat{X}_{k|k-1}^{(0)}$  stands for the agent's state prediction at a time  $k$  given the corrected state at the instant  $k-1$ , i.e.,  $\hat{X}_{k-1|k-1}^{(0)}$ .

Innovations are quantities that measure the deviation that a proposed dynamical model presents from observations. In the ideal case,  $\tilde{Y}_k^{(0)}$  tends to zero, which indicates that the utilized dynamic model explains the observed agent's motions precisely. Following this reasoning, when innovations are significantly different from zero, the proposed dynamical model should be modified to describe more accurately the observed agent's motions. In such cases, effects are added as a term  $BU_{(l),k}$  as proposed in equation (7).

Let **(1)** index the estimations made by a dynamical model based on equation (7). By supposing a null innovation produced by such model, i.e.,  $\tilde{Y}_k^{(1)} = 0$ , it is assumed that the new motivated model describes data perfectly, such that:

$$Z_k - H \hat{X}_{k|k-1}^{(1)} = 0. \quad (11)$$

By considering that predictions made by the non-motivated model follow the next property:  $\hat{X}_{k|k-1}^{(0)} \sim \hat{X}_{(0)k-1|k-1}^{(0)}$ ; due to low Gaussian process noise  $w_k^{(l)}$ , it is possible to write:

$$\hat{X}_{k|k-1}^{(1)} \sim \hat{X}_{k|k-1}^{(0)} + BU_k. \quad (12)$$

Furthermore, by replacing (12) in (11), it is possible to obtain an approximation of the control vector  $U_k$  through some calculations, such that:

$$HBU_k \sim Z_k - H \hat{X}_{k|k-1}^{(0)} = \tilde{Y}_k^{(0)} \Rightarrow U_k \sim \frac{\tilde{Y}_k^{(0)}}{\Delta k}. \quad (13)$$

From equation (13), it is possible to see how innovations (from non-motivated models) approximate the agents' velocities (motivated actions). By including such term in equation (7), it is possible to rewrite the motivated model as:

$$X_{(l),k+1} = FX_{(l),k} + B \left( \frac{\tilde{Y}_{(l),k}^{(0)}}{\Delta k} \right) + w_k^{(l)}. \quad (14)$$

The built dynamic model shown in (14) can be used for tracking agents whose current state is  $X_{(l),k}$ . Sparse observed positions of an agent  $l$  can be written as  $H X_{(l),k}^A$  (GP inputs) and their correspondent displacements as  $\tilde{Y}_{(l),k}^{(0),A}$  (GP outputs), where  $A$  represents an activity, i.e., moving pattern in the scene. By using such data to approximate the function  $\hat{g}_A(\cdot)$ , it is possible to rewrite equation (14) as follows:

$$X_{(l),k+1} = FX_{(l),k} + B \hat{g}_A(H X_{(l),k}^A) + w_k^{(l)}. \quad (15)$$

The following section explains in detail the nonparametric methodology for obtaining  $\hat{g}(\cdot)$  from observed location data.

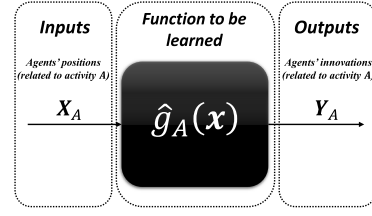


Fig. 2. General scheme for supervised learning of spatial-velocity relationships for an activity  $A$ .

### B. Gaussian Process Application

Based on the local linear dynamical models calculated previously, this step aims at generalizing such models through the whole environment. Let  $\mathcal{X}_A = H X^A$  be a vector consisting of a set of positions related to a given task indexed as  $A$ . Additionally, let  $\mathcal{Y}_A = \tilde{Y}^{(0),A}$  be a vector of the same size of  $\mathcal{X}_A$  containing the respective innovations obtained from the non-motivated model, see equation (10). Accordingly, by considering  $\mathcal{X}_A$  and  $\mathcal{Y}_A$  data, it is possible to use supervised learning for estimating a function  $\hat{g}(\cdot)$  that relates them. Fig. 2 shows the main idea of such a learning process.

By taking the sparse space locations  $\mathcal{X}_A$  (inputs) and their corresponding measured innovations from the non-motivated model  $\mathcal{Y}_A$  (outputs), it is possible to use a GP regression that estimates the agents' motion (expected innovations) for all points in the environment when they perform a particular activity  $A$ . The following expression shows the GP regression considered in the proposed approach:

$$\mathcal{Y}_A = \hat{g}_A(\mathcal{X}_A) + \nu_A, \quad (16)$$

$\hat{g}_A(\cdot)$  takes agent's locations as inputs and estimates their expected motions (at such positions) for an activity  $A$ . In addition,  $\nu_A \sim \mathcal{N}(0, \sigma_A^2)$  is a Gaussian zero-mean white noise process. Since agents' motions are assumed to be similar at a given location when they execute a particular activity, a local Gaussian noise assumption turns out to be adequate for describing uncertainties in proposed dynamical models. Consistently,  $\hat{g}(\cdot)$  is distributed as a GP defined by its mean and covariance functions, see section III. In this work, a linear mean and a squared exponential kernel functions are considered to perform GP estimations. Equation (17) shows the squared exponential kernel function.

$$\kappa(\mathcal{X}_1, \mathcal{X}_2) = \phi^2 e^{-\frac{\|\mathcal{X}_1 - \mathcal{X}_2\|^2}{2\phi^2}}, \quad (17)$$

where  $\phi^2$  denotes the global variance of the mapping; and  $\phi^2$  is the global smoothness parameter of the estimation. The employed kernel (covariance) allows the GP to model arbitrary nonlinear functions.

### C. Gaussian Process Codification

Innovations estimated from the GP regression are projected on a uniformed discrete location map of the environment. In this way, GP results are discretized into three types of information: (i) Spatial grid,  $\mathfrak{X}_A$ , which corresponds to the scene points where the GP is evaluated. (ii) Innovation grid,  $\mathfrak{Y}_A$ , which approximates the most probable motion at each

evaluated position  $\mathbf{x} \in \mathfrak{X}_A$ . (iii) Uncertainty grid,  $\mathfrak{y}_A$ , which codifies the validity of GP estimations. Accordingly, each grid data related to an activity  $A$  can be written as:

$$\begin{aligned}\mathfrak{X}_A &= \{\mathcal{X}_{A,1}, \mathcal{X}_{A,2}, \dots, \mathcal{X}_{A,q}, \dots, \mathcal{X}_{A,Q-1}, \mathcal{X}_{A,Q}\}, \\ \mathfrak{Y}_A &= \{\mathcal{Y}_{A,1}, \mathcal{Y}_{A,2}, \dots, \mathcal{Y}_{A,q}, \dots, \mathcal{Y}_{A,Q-1}, \mathcal{Y}_{A,Q}\}, \\ \mathfrak{v}_A &= \{v_{A,1}, v_{A,2}, \dots, v_{A,q}, \dots, v_{A,Q-1}, v_{A,Q}\}.\end{aligned}$$

where  $\mathcal{X}_{A,q}$ ,  $\mathcal{Y}_{A,q}$  and  $v_{A,q}$  represent respectively input, output and uncertainty estimated information, see equation (16), associated with the grid point indexed as  $q$ .  $Q$  is the total number of cells that discretize the GP results.

The uncertainty grid  $\mathfrak{y}_A$  serves to identify GP estimations that tend to be imprecise according to the training data. The GP noise of a grid point  $q$  can be represented as a Gaussian distribution  $v_{A,q} \sim \mathcal{N}(0, \sigma_{A,q}^2)$ . Since an environment of  $d$  dimensions is considered,  $\sigma_{A,q}^2$  is a  $d \times d$  covariance matrix whose diagonal encodes the precision of GP estimations.

Motivated by the work proposed in [19], for each grid point it is considered a joint uncertainty vector that unifies variances obtained for the  $d$  dimensions of environment, such that:

$$\xi_{A,q} = \sum_{i=1}^d (\sigma_{A,q(i)}^2), \quad (18)$$

where  $\sigma_{A,q(i)}^2$  represents the  $i$ -th diagonal component of the covariance matrix  $\sigma_{A,q}^2$ . Let  $\mathfrak{s}_A$  be the set of joint uncertainties associated to an activity  $A$ , such that:

$$\mathfrak{s}_A = \{\xi_{A,1}, \xi_{A,2}, \dots, \xi_{A,q}, \dots, \xi_{A,Q-1}, \xi_{A,Q}\}.$$

Additionally, let  $\mathfrak{s}_A^*$  be the normalized version of the vector  $\mathfrak{s}_A$ , such that components of  $\mathfrak{s}_A^*$  belong to the interval  $[0, 1]$ . Such normalization process facilitates to approximate a beta probability distribution  $\mathfrak{B}_A = \text{beta}(\alpha_A, \beta_A)$  that fits the data in  $\mathfrak{s}_A^*$ . Consequently, by analyzing the cumulative distribution function of  $\mathfrak{B}_A$ , it is possible to remove the grid points that carry high uncertainty information. A cumulative probability threshold  $\lambda_{val} \in [0, 1]$  is fixed for such task. Accordingly, grid points associated with  $CDF(\mathfrak{B}_A) > \lambda_{val}$  are removed in succeeding analyses.  $CDF(\mathfrak{B}_A)$  represents the cumulative density function of the distribution  $\mathfrak{B}_A$ .

Let  $\mathfrak{X}_{A,\lambda_{val}}$ ,  $\mathfrak{Y}_{A,\lambda_{val}}$  and  $\mathfrak{v}_{A,\lambda_{val}}$  be the valid GP grid data obtained by fixing a  $\lambda_{val}$  value. Note that as  $\lambda_{val}$  approaches 0, fewer valid grid points are generated. Larger  $\lambda_{val}$  values produce a greater number of valid GP data.

#### D. Identification of Dynamic Zones

After obtaining valid GP estimated data, i.e.,  $\mathfrak{X}_{A,\lambda_{val}}$ ,  $\mathfrak{Y}_{A,\lambda_{val}}$  and  $\mathfrak{v}_{A,\lambda_{val}}$ , it is proposed to detect large spatial zones where agents' innovations are quasi-constant such that linear dynamic models can be applied for tracking purposes. This paper adopts an OS method from which larger zones are extracted by a region growing procedure.

1) *Superpixel Over-Segmentation*: A superpixel algorithm proposed by [41] is employed to discretize valid grid data into space regions where innovations are strictly similar. Accordingly, it is obtained a total of  $N$  clusters (regions) that discretize vectors  $\mathfrak{X}_{A,\lambda_{val}}$ ,  $\mathfrak{Y}_{A,\lambda_{val}}$  and  $\mathfrak{v}_{A,\lambda_{val}}$ .

Uncertainty grid points  $\mathfrak{y}_{A,\lambda_{val}}$  are not taking into consideration as an input parameter for segmenting data. Since valid data is already obtained based on such information, it is assumed that  $\mathfrak{y}_{A,\lambda_{val}}$  does not influence the cluster generation.

As explained in [41], superpixel algorithms are based on a similarity function between two spatial points  $p_1$  and  $p_2$ :

$$W(p_1, p_2) = C_X^2 \cdot W_X(p_1, p_2) + C_Y^2 \cdot W_Y(p_1, p_2). \quad (19)$$

In this work, both points  $(p_1, p_2)$  are assumed to be part of the valid grid spatial data, i.e.,  $\{p_1, p_2\} \in \mathfrak{X}_{A,\lambda_{val}}$ . Parameters  $C_X$  and  $C_Y$  control the relative significance of similar values in vectors  $\mathfrak{X}_{A,\lambda_{val}}$  and  $\mathfrak{Y}_{A,\lambda_{val}}$  respectively.  $W_X(\cdot, \cdot)$  and  $W_Y(\cdot, \cdot)$  are functions that take a couple of spatial points  $(p_1, p_2)$  and calculate the difference between their location and velocity information respectively, such that:

$$\begin{aligned}W_X(p_1, p_2) &= d - \|\mathcal{X}_{A,p_1}^{\lambda_{val}} - \mathcal{X}_{A,p_2}^{\lambda_{val}}\|_2^2 \\ W_Y(p_1, p_2) &= d - \|\mathcal{Y}_{A,p_1}^{\lambda_{val}} - \mathcal{Y}_{A,p_2}^{\lambda_{val}}\|_2^2,\end{aligned} \quad (20)$$

where  $\mathcal{X}_{A,p}^{\lambda_{val}}$  and  $\mathcal{Y}_{A,p}^{\lambda_{val}}$  represent respectively the normalized position and velocity information associated to the valid point  $p$ , such that  $\mathcal{X}_{A,p}^{\lambda_{val}} \in \mathfrak{X}_{A,\lambda_{val}}$  and  $\mathcal{Y}_{A,p}^{\lambda_{val}} \in \mathfrak{Y}_{A,\lambda_{val}}$ .  $d$  is the number of dimensions of the environment. As pointed out by [41], the vital metric to adjust is the ratio  $r$ , defined as:

$$r = \frac{C_X}{C_Y}, \quad (21)$$

The expected number of regions  $\hat{N}$  is a key parameter to set in superpixel algorithms. In an OS process, the number of regions is maximized for given a ratio  $r$ . A high value of  $\hat{N}$  guarantees an OS version of vectors  $\mathcal{X}_{A,p}^{\lambda_{val}}$  and  $\mathcal{Y}_{A,p}^{\lambda_{val}}$ .

The final result of this stage consists of a set of  $N$  spatial zones where agents' innovation values are quasi-constant. Each generated region can be seen as a cluster of location and innovation data samples taken from valid information  $\mathfrak{X}_{A,\lambda_{val}}$  and  $\mathfrak{Y}_{A,\lambda_{val}}$ . Accordingly, each region is composed of two sets of data, such that:

$$\begin{aligned}\mathfrak{C}_{\mathcal{X},n}^A &= \{\mathcal{X}_{A_n,1}^{\lambda_{val}}, \mathcal{X}_{A_n,2}^{\lambda_{val}}, \dots, \mathcal{X}_{A_n,m_n}^{\lambda_{val}}, \dots, \mathcal{X}_{A_n,M_n}^{\lambda_{val}}\} \\ \mathfrak{C}_{\mathcal{Y},n}^A &= \{\mathcal{Y}_{A_n,1}^{\lambda_{val}}, \mathcal{Y}_{A_n,2}^{\lambda_{val}}, \dots, \mathcal{Y}_{A_n,m_n}^{\lambda_{val}}, \dots, \mathcal{Y}_{A_n,M_n}^{\lambda_{val}}\}\end{aligned} \quad (22)$$

where  $m_n$  indexes the elements belonging to the region  $n$ . Additionally,  $\mathcal{X}_{A_n,m_n}^{\lambda_{val}} \in \mathfrak{X}_{A,\lambda_{val}}$  and  $\mathcal{Y}_{A_n,m_n}^{\lambda_{val}} \in \mathfrak{Y}_{A,\lambda_{val}}$ .  $M_n$  is the total number of clustered data into the region  $n$ .

Let  $\mu_{\mathcal{X},n}^A$  and  $\mu_{\mathcal{Y},n}^A$  be vectors containing the average value of clustered positions and innovation components respectively. Moreover, let  $\tilde{\sigma}_{A,n}^2$  be a vector containing the variances of clustered innovation components. Lastly, let  $\tilde{\sigma}_{A,n(\text{sum})}^2$  be the summation of variance components encoded in  $\tilde{\sigma}_{A,n}^2 \cdot \tilde{\sigma}_{A,n(\text{sum})}^2$  measures the level of linearity associated with the dynamical model in region  $n$ . Low values of  $\tilde{\sigma}_{A,n(\text{sum})}^2$  indicate coherent innovation evidence that supports the validity of a quasi-linear model in the region  $n$ .

By considering the spatial vicinity between clustered regions, it is possible to build a graph structure which encodes the location connectivity between generated regions. Accordingly, the graph's nodes represent obtained clusters, whereas edges encode spatial connections between the regions.

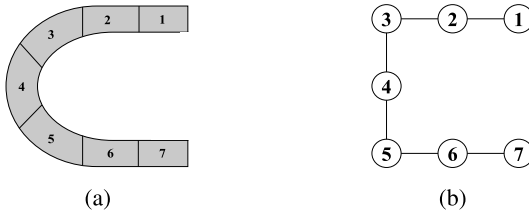


Fig. 3. Example of generated regions and graph equivalence. (a) Superpixel generated regions. (b) Graph version of zones.

Fig. 3 shows a straightforward example of 7 generated zones connected spatially one after the other.

By applying an edge contraction operation on the super-pixel's graph equivalence of obtained regions, it is possible to achieve spatial broader areas where quasi-linear motion models are still valid. As mentioned before, such a process facilitates the obtainment of extended regions containing consistent innovation information. A region growing procedure is employed for generating such broader zones which are used later for prediction and detection of abnormalities.

2) *Region Growing Process*: As mentioned previously, obtained regions can be mapped into a graph whose nodes contain information about average locations, i.e.,  $\mu_{\mathcal{X},n}^A$ , dynamical models, i.e.,  $\mu_{\mathcal{Y},n}^A$ ; and their validity, i.e.,  $\tilde{\sigma}_{A,n}^2$ .

Dynamical models can be described as a multivariate Gaussian distribution that is built based on mean values  $\mu_{\mathcal{Y},n}^A$  and variances  $\tilde{\sigma}_{A,n}^2$ . A distance measurement  $\varepsilon_{n_1,n_2}$  between two adjacent regions  $n_1$  and  $n_2$  is considered to merge obtained zones, such that:

$$\varepsilon_{n_1, n_2} = \sum_{i=1}^d D_B(P_{n_1}^i, P_{n_2}^i), \quad (23)$$

where  $D_B(p, q)$  indicates the Bhattacharyya distance between a couple of Gaussian distributions  $p$  and  $q$ .  $P_{n_1}^i$  and  $P_{n_2}^i$  are Gaussian distributions of spatially adjacent regions ( $n_1$  and  $n_2$ ) related to the  $i$ -th dimension of the scene. As specified before, such Gaussian distributions are defined based on the mean and variance values in vectors  $\mu_{\mathcal{Y}, n}^A$  and  $\tilde{\sigma}_{A, n}^2$  respectively. Additionally, let  $n_{conn}$  be a vector containing the set of regions that are spatially adjacent to the region  $n$ . Accordingly, in equation (23),  $n_2 \in n_{1conn}$  and  $n_1 \in n_{2conn}$ .

By considering a threshold value  $\varepsilon_{\lambda_{bhat}}$  for merging adjacent regions, it is possible to obtain larger zones where quasi-linear models are still valid. For fixing  $\varepsilon_{\lambda_{bhat}}$ , it is considered the Bhattacharyya distances (equation (23)) between all adjacent regions. Such distances are normalized into the interval  $[0, 1]$ ; and a beta probability distribution  $\mathfrak{B}_{bhat, A}$  is approximated based on such information. As it is well known, a beta cumulative distribution evaluated in the point  $\varepsilon_{\lambda_{bhat}}$  provides the probability of obtaining values in the interval  $[0, \varepsilon_{\lambda_{bhat}}]$ . Let us define such probability as  $\lambda_{bhat}$ . Consistently, since the proposed distribution encodes distances between regions, probability values  $\lambda_{bhat} \sim 0$  codify similar regions whereas  $\lambda_{bhat} \sim 1$  capture large differences between zones. By fixing a threshold probability  $\lambda_{bhat} \in [0, 1]$ , a maximum threshold distance  $\varepsilon_{\lambda_{bhat}}$  that favors the most similar distances between

---

**Algorithm 1** Region merging process

## Input:

- 1:  $[\mu_{Y,n}^A]$  Mean values of innovations in regions
  - 2:  $[\tilde{\sigma}_{A,n}^2]$  Variance of innovation components in regions
  - 3:  $[n_{conn}]$  Spatial connectivity between all regions
  - 4:  $[\varepsilon_{\lambda, phat}]$  Threshold value to fuse regions
  - 5:  $[\tilde{\sigma}_{A,n(sum)}^2]$  Uncertainty of regions' models

## Output:

- ```

6: [ $\tilde{\sigma}_{A,n^*}^2$ ;  $\mu_{\mathcal{X},n^*}^A$ ;  $\mu_{\mathcal{Y},n^*}^A$ ] Merged regions' properties
7: procedure REGION GROWING
8:   Initialization:  $\mu_{\mathcal{X},n^*}^A \leftarrow \mu_{\mathcal{X},n}^A$ ;  $\mu_{\mathcal{Y},n^*}^A \leftarrow \mu_{\mathcal{Y},n}^A$ 
9:    $\tilde{\sigma}_{A,n^*}^2 \leftarrow \tilde{\sigma}_{A,n}^2$ ;  $\tilde{\sigma}_{A,n^*(sum)}^2 \leftarrow \tilde{\sigma}_{A,n(sum)}^2$ 
10:  loop:
11:   $n_i \leftarrow$  Region with the lowest uncertainty in  $\tilde{\sigma}_{A,n^*(sum)}^2$ 
12:   $n_{i_{min}} \leftarrow$  Region connected to  $n_i$  with the minimum
13:    uncertainty value
14:  if ( $\varepsilon_{n_i, n_{i_{min}}} < \varepsilon_{\lambda_{bhat}}$ ) == TRUE then
15:     $n_{new} \leftarrow$  Region resulting from merging
16:     $n_i$  and  $n_{i_{min}}$ 
17:    Update [ $\mu_{\mathcal{X},n^*}^A$ ;  $\mu_{\mathcal{Y},n^*}^A$ ;  $\tilde{\sigma}_{A,n^*}^2$ ;  $\tilde{\sigma}_{A,n^*(sum)}^2$ ] by
18:    removing  $n_i$  and  $n_{i_{min}}$  data and adding  $n_{new}$ 
19:  else
20:    Eliminate  $n_i$  data from  $\tilde{\sigma}_{A,n^*(sum)}^2$ 
21:  goto loop Until resulting regions cannot be merged
22:                                among them anymore.

```

regions, i.e., values in the interval  $[0, \varepsilon_{\lambda_{bhat}}]$ , is implicitly defined.

Couples of regions  $n_1$  and  $n_2$  that produce a distance measurement of the type  $\varepsilon_{n_1,n_2} < \varepsilon_{\lambda_{hat}}$  are incrementally merged such as indicated in Algorithm 1. The final result of this stage consists of larger regions that will be used for prediction and abnormality detection purposes.

The diagram in Fig. 4 summarizes the steps explained through sections IV-A, IV-B, IV-C and IV-D.

### E. DBN Representation

By taking the grown regions properties previously calculated as input data, this step generates a probabilistic inference architecture that facilitates the tracking of future agents. A Dynamical Bayesian Network (DBN) architecture is employed to represent the motion of observed agents in an environment. DBNs enable to include dependencies between involved random variables as time evolves. DBNs facilitate the representation of different inference levels related to agents' dynamics and incorporate the variables' uncertainties when predicting future instances. In this paper, the lowest level of inference corresponds to measurements  $Z_k$ . States of agents,  $X_k$ , represent a medium inference level which captures continuous information of agents. Super-states  $A_k$  and  $n_k$  correspond to the top level of inference, which consists of the complete activity that an agent performs  $A_k$  together with its respective discretization of regions  $n_k \in n^*$ ; where  $n^*$  represents the set of large areas obtained from Algorithm 1. In such a top level, activities can be seen as a set of discrete sub-tasks executed one after the other. Each sub-tasks is described as

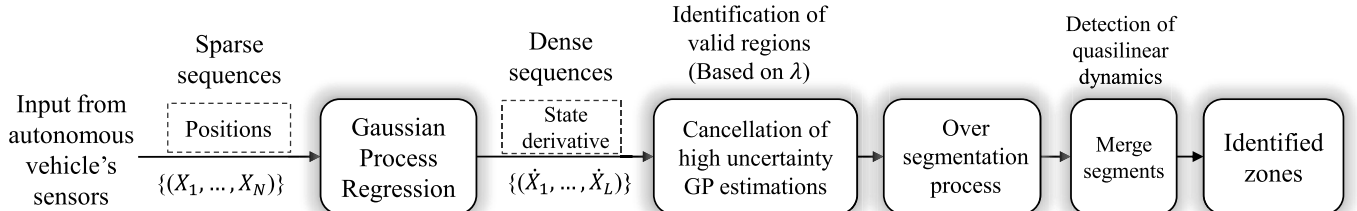


Fig. 4. Block diagram of the proposed methodology for detecting elemental dynamical zones.

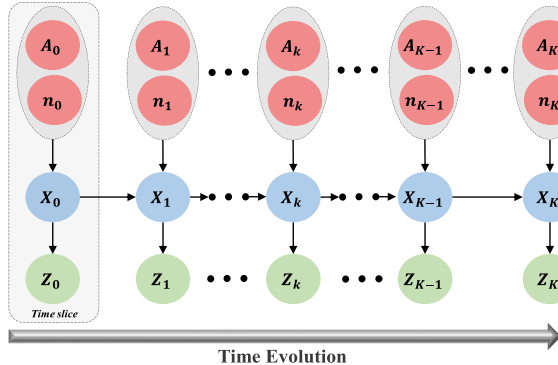


Fig. 5. Proposed DBN architecture for modeling abnormalities.

linear models which define the expected dynamics of agents according to their location in the environment.

Fig. 5 depicts the employed DBN architecture. Each inference level is identified with a different color and arrows represent dependencies between variables. A dotted rectangle represents a single time instant  $k$  where the three levels are related to each other through conditional dependencies. The proposed DBN assumes that observations are continuous position values that can be modeled as Gaussian distributions. Similarly, agents' states are modeled as a multivariate normal distribution that carries information related to the positions and time derivatives of the agent in question.

From Fig. 5, it is possible to see that each time slice of the proposed representation involves three conditional dependencies: (i)  $p(Z_k|X_k)$  which is the probability of obtaining an observation given the agent's state. This work considers the measurement model shown in equation 6 for making such inference. (ii)  $p(X_{k+1}|X_k)$  which represents the probability of obtaining a future agent's state given its present one. The proposed approach considers the transition model discussed in equation (15) to make the inference in question. (iii)  $p(X_k|A_k, n_k)$  that expresses the probability of having the agent's state  $X_k$  given the super-state  $n_k$  related to the activity  $A_k$ . Let  $x_{n_k}$  be the spatial components covered by the region  $n_k$  and  $\dot{x}_{n_k}$  be their correspondent quasi-constant velocity components. Note that mean values of the last two variables belong to the set of properties related to regions' spatial centroids and dynamical models calculated in Algorithm 1, such that  $\bar{x}_{n_k} \in \mu_{\mathcal{X}, n^*}^A$  and  $\bar{\dot{x}}_{n_k} \in \mu_{\mathcal{Y}, n^*}^A$ .

Since  $n_k$  fixes a specific dynamical model, it is possible to approximate the control input in equation (15) as:

$$\hat{g}_{A_k}(HX_{(l),k}) \simeq \bar{x}_{n_k}, \quad (24)$$

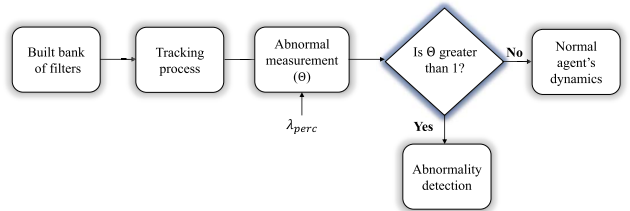


Fig. 6. Proposed steps for detecting abnormalities.

where it is assumed that  $H X_{(l),k} \in \mathbf{x}_{n_k}$ . As can be seen from equation (24), by knowing the agent's current region  $n_k$ , it is possible to approximate the function  $g_{A_k}$  as the region's mean velocity components of the proposed discretization process.

Proposed DBNs depend on the previous state information for predicting future instances. Since the state of an agent  $(l)$  is composed if its positions and  $m$  time derivatives, such that  $X_{(l)} = [\mathbf{x}_{(l)} \ \dot{\mathbf{x}}_{(l)} \ \cdots \ \mathbf{x}_{(l)}^{(m)}]^T$ , by increasing the number of derivatives  $m$ , more information from the past is considered when making predictions. This paper only considered the agents' velocity, i.e.,  $m = 1$ , as part of the states. Such a choice assumes a sampling time that enables to capture the agents' motions and approximate them as piecewise constant velocity models. Our DBNs can be seen as hierarchical structures containing both model selection and state estimation.

#### F. Abnormality Detection

Since the aim of this work is to conduct abnormality detection based on probabilistic inferences. Fig. 6 summarizes the abnormality detection process for analyzing new unseen behaviors/maneuvers of agents in an environment.

Our method uses a set of KFs to track agents' continuous states  $X_k$  based on models in regions  $n^*$ . This work considers a switching KF approach based on locally linear models previously obtained in Algorithm 1. As shown in Fig. 7, proposed KFs are built based on identified regions' information.

The proposed approach is based on local linear models, see in equation (15), where control inputs are modeled as shown in equation (24). KFs employ such models for predicting agents' future states. The error of such predictions can be used to build a normality indicator of observed agents' motions.

KFs' error is defined as the innovations generated by all created (normal) filters valid in the current agent's location. As mentioned previously, each region's model can be seen as a multivariate Gaussian distribution defined by expected velocities,  $\mu_{\mathcal{X}, n}^A$ ; and their variances,  $\tilde{\sigma}_{A, n}^2$ ; where  $n \in n^*$ . By determining a percentage threshold  $\lambda_{perc} \in [0, 1]$  that

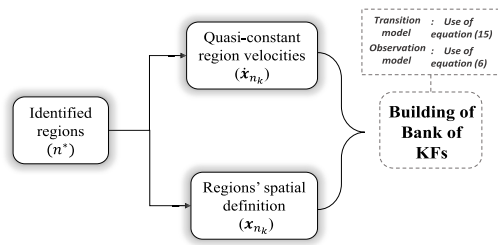


Fig. 7. Proposed building of KFs for switching purposes.

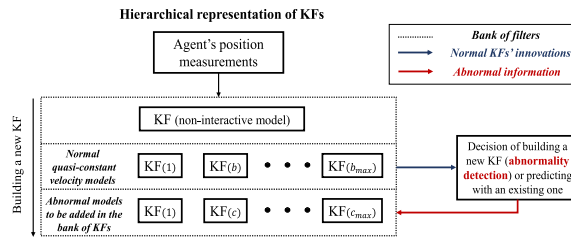


Fig. 8. Scheme of abnormality detection.

establishes the normality limits of observed dynamics, it is possible to obtain the vector  $\Delta \tilde{Y}_{n(\text{perc})}$  containing the maximum allowed deviations from expected dynamics  $\mu_{\mathcal{X},n}^A$ . Let  $\theta_{n_k}$  be the KF's innovations divided by the maximum allowed deviations in the region  $n_k \in n^*$ , such that:

$$\theta_{n_k} = \frac{\text{abs}(\tilde{Y}_k)}{\Delta \tilde{Y}_{n(\text{perc})}}. \quad (25)$$

Note that  $\theta_{n_k}$  is a vector that includes the normalized innovations of the  $d$  components of the scene. The final abnormality measure is defined as the maximum value of such vector:

$$\Theta_k = \max(\theta_{n_k}). \quad (26)$$

Abnormal dynamics can be identified automatically by the proposed method when the abnormality measurement  $\Theta_k$  is greater than 1; whereas the normal dynamics are inside the range [0, 1]. Accordingly, observations detected as abnormal can be used to create ulterior linear models that can be added into the set of KFs. Such a process allows the system to learn new (abnormal) models incrementally and use them in future instances for prediction and tracking purposes. Fig. 8 shows how ulterior KFs can be represented into a hierarchical scheme. Normal KFs employed for detecting abnormalities are indexed as  $b$ , whereas anomalies which can be potentially added into new KFs models indexed as  $c$ .

Results of this work focus on the identification of abnormal situations that can be integrated into a set of KFs incrementally. In our approach, abnormalities are associated with the system's incapacity of explaining observations based on previously characterized models. The whole proposed method is tested with real measurements taken from a vehicle that performs diverse tasks in a closed environment. The following section described the employed dataset in detail.

## V. EMPLOYED DATASET

A real vehicle [45], shown in Fig. 9a is employed for testing the proposed algorithms. A human expert drives the vehicle

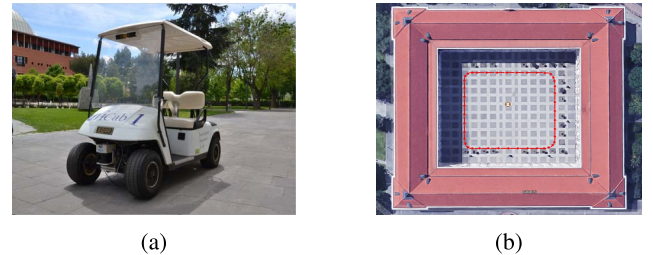


Fig. 9. Observed moving agent and closed scene. (a) Autonomous vehicle "iCab". (b) Closed environment.

performing some tasks in a closed environment. Accordingly, a control perimeter task is first executed; and from it, two other situations are contemplated.

Sensory data used in this work consists of vehicle's positions mapped into Cartesian coordinates provided by an odometry manager. Velodyne point-cloud data (taken from ROS data [46]) is processed to generate a 2-dimensional ( $x, y$ ) measurement of the vehicle's location inside the environment, see Fig. 9b. Obtained odometry data has an accuracy of around 10 cm. Additionally, an error of 0.5 degrees is considered due to the data acquisition process [47]. Due to the considerable computational cost of the point cloud processing, a separated computer is necessary. A software prototyping tool named ROS [46] is responsible for the communication between processes and computers.

A perimeter monitoring (PM) activity is first considered as a vehicle's baseline task. From such activity, two abnormal situations are contemplated. The three different scenarios, i.e., standard PM and two anomalies while executing it, are described as follows

**Scenario I (perimeter monitoring):** The vehicle performs a rectangular path surrounding a closed environment, see the red trajectory in Fig. 9b.

**Scenario II (avoidance maneuver):** While the vehicle executes a perimeter monitoring task, two static pedestrians are placed in different locations interfering with its path. In this scenario, the vehicle performs an avoidance maneuver to surpass the static pedestrian and continues the PM activity. Fig. 10 shows the temporal evolution of the avoidance maneuver from a first-person perspective. As can be seen, when the vehicle observes a static pedestrian, it surrounds him and then continues its trajectory.

**Scenario III (stop maneuver):** While the vehicle executes a perimeter monitoring task, it encounters in each lap two moving pedestrians that cross in front of its path. In such encounters, the vehicle's reaction consists of an emergency stop maneuver; then it continues its regular path as soon as the pedestrian leaves its field of view. A vehicle's first-person perspective of the temporal evolution of the stop maneuver is provided in Fig. 11.

Each scenario consists of 20 laps around the environment. Location data of each case is analyzed in the following section.

## VI. RESULTS

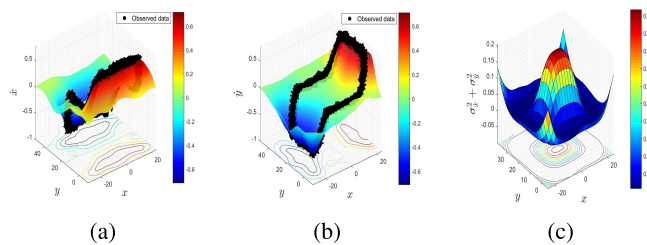
As mentioned before, three main scenarios are considered: (i) perimeter monitoring task, (ii) Avoidance maneuver while



Fig. 10. Pedestrian avoidance situation.



Fig. 11. Emergency stop situation.

Fig. 12. GP regression based on innovations produced by the perimeter control scenario: Normality definition. (a) GP over  $x$  data. (b) GP over  $y$  data. (c) GP uncertainty.

performing PM and (iii) Emergency stop while executing PM. Unseen maneuvers, i.e., situations in (ii) and (iii) represent abnormalities from the regular PM task.

**Threshold Setting:** The proposed method requires the setting of three threshold values, each of them already discussed in section IV. For the experiments shown in this article, each of them is set as follows: (i)  $\lambda_{val} = 0.7$  which selects the most certain grid points to be analyzed by the proposed method (ii)  $\lambda_{bhat} = 0.7$  which facilitates the merging of similar neighbor OS regions and (iii)  $\lambda_{perc} = 0.9$ , which enables the recognition of abnormal motions based on deviations from previously learned models. It was observed that values higher than 0.5 do not reject relevant data for generating the DBN.

#### A. Normality Characterization: A GP Approach

Based on trajectories that describe the PM activity, see the red path in Fig. 9b, it is applied a GP regression that follows the inputs/outputs of Fig. 2. Innovation components  $\dot{x}$  and  $\dot{y}$ , approximated by the GP and mapped into coordinate positions  $(x, y)$  are presented in Figs. 12a and 12b respectively.

As proposed in equation (18), uncertainty values generated by innovation components are summed up to obtain an uncertainty measure in each environment location. A resulting surface containing coupled uncertainties of GP estimations onto the whole scene is shown in Fig. 12c.

As explained in section IV-D, an OS superpixel algorithm is applied over valid GP estimations, i.e.,  $\mathfrak{X}_{A,\lambda_{val}}$ ,  $\mathfrak{Y}_{A,\lambda_{val}}$  and  $\mathfrak{y}_{A,\lambda_{val}}$ . Fig. 13a shows the result of OS superpixels for the PM task. Subsequently, by applying the region growing approach,

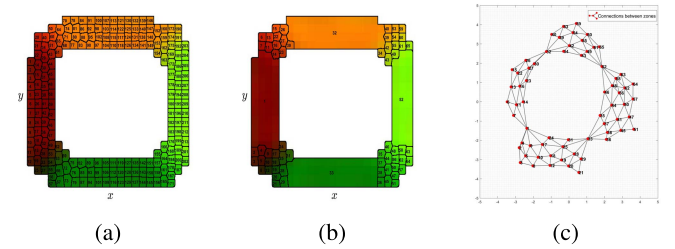


Fig. 13. Segmentations of GP perimeter control information into zones where quasi-constant velocity models are valid. (a) OS version. (b) Grown regions. (c) Graph version.

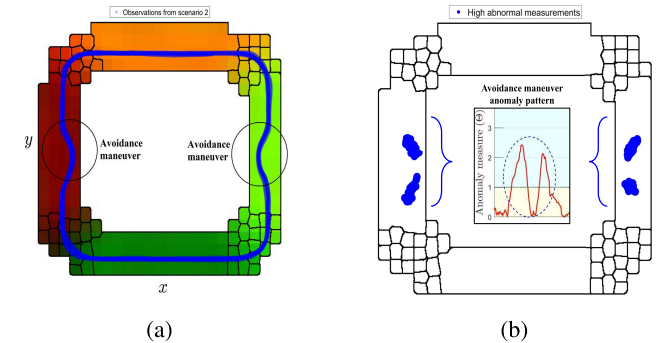


Fig. 14. Avoidance maneuver data and anomaly results. (a) Avoidance maneuver data. (b) Identified anomalies.

see Algorithm 1, large regions where quasi-constant velocity models are valid can be obtained, see Fig. 13b.

#### B. Abnormality Detection of Unseen Maneuvers

Each region in Fig. 13b is employed to create a KF valid in the spatial zone in question. Fig. 13c presents a graph that encodes the connections between produced zones. As can be seen, 64 regions are obtained and used for tracking purposes. In other words, our method decomposes the PM task into 64 linear dynamical models extracted from GP valid data, see section IV-D. Additionally, as explained in section IV-E, each linear dynamical model is employed into a motivated KF for prediction and abnormality detection purposes, see equations (15) and (24).

Both types of unseen maneuvers, i.e., avoidance and emergency stop, are analyzed based on models learned with PM experiences (normal data).

*1) Static Pedestrian Avoidance:* Fig. 14a shows in blue the measured locations of a vehicle that performs two avoidance maneuvers during the PM task. The background colored image displays the identified regions where quasi-constant velocity models are valid based on the regular PM task.

By considering innovations generated by the set of KFs based on the PM task (normality), it is possible to identify abnormalities in new trajectory data that does not correspond to already learned models. As explained previously, high innovation values from KFs indicate the presence of anomalies in the scene. Since this work considers a 2-dimensional environment, two values of innovations are obtained at each time instant  $k$ . As shown in (25), the vector  $\theta_{nk}$  is obtained

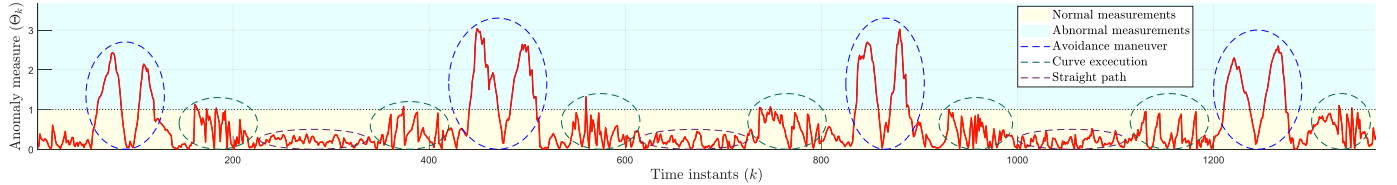


Fig. 15. Abnormality measurements through time for perimeter control activity with avoidance of static pedestrians.

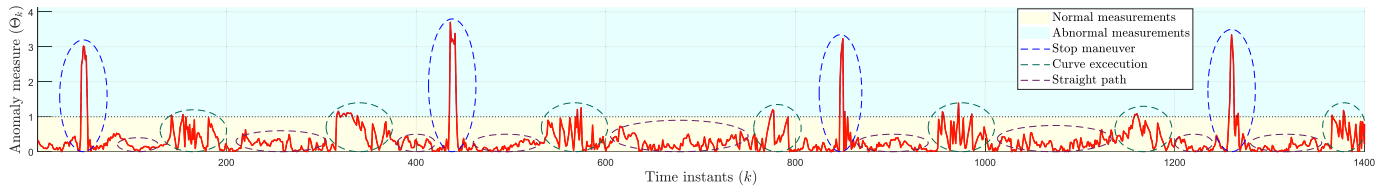


Fig. 16. Abnormality measurements through time for perimeter control activity with emergency stop maneuver.

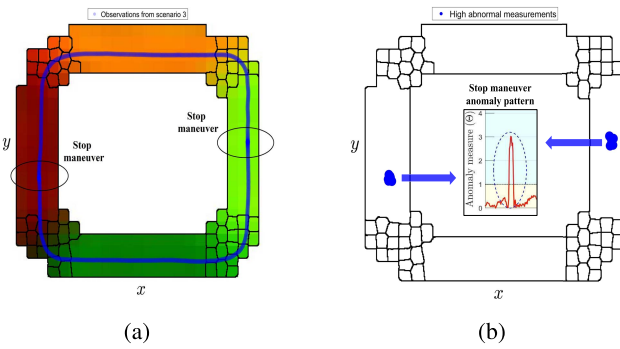


Fig. 17. Stop maneuver data and anomaly results. (a) Stop maneuver data. (b) Identified anomalies.

by taking the absolute value of innovations and normalizing them according to the maximum allowed deviations. The final anomaly measurement consists of the highest value of the vector  $\theta_{nk}$ , see equation (26). Accordingly, Fig. 15 presents the anomaly measure  $\Theta_k$  through time obtained by applying the normal PM model to observations from scenario II.

Three main behaviors are recognized in the time series presented in Fig. 15, they correspond to “avoiding maneuver”, “curve execution” and “straight path”. As can be seen, parts of the avoidance maneuver and few points of the curve execution are detected as abnormal, i.e.,  $\Theta_k \geq 1$ . Since avoidance maneuvers were not observed before, it is understandable that they produce high peaks of abnormality in points where the vehicle was supposed to go in a straight path. Curve points that present high anomaly values correspond to parts of the turns that do not assemble precisely with the maneuvers observed previously. Nonetheless, note that curves do not produce significantly abnormal measurements as avoidance maneuvers do.

It is relevant to mention that the anomaly pattern related to the avoidance maneuver, i.e., abnormal measurements inside blue ovals in Fig. 15, is space independent. In other words, if there is an avoidance in any other large region of the environment (e.g., 1, 32, 33 and 52 shown in Fig. 13b), a similar pattern will appear as it occurs. Additionally, note

that straight path motions are identified clearly as normal behaviors concerning the standard perimeter control task.

Fig. 14b shows observations of scenario II that produced high abnormalities when using PM experiences for building the inference models. Two anomaly zones are obtained each time that an avoidance maneuver is performed. A single compact zone (in blue) is not formed due to the straight path in the avoidance maneuver, which follows the regular PM task. Position and displacement information related to anomaly zones shown in Fig 14b can be included in the current bank of filters as proposed in the scheme displayed in Fig. 8.

2) *Emergency Stop Maneuver:* Fig. 17a shows in blue the vehicle’s locations while executing PM with two stop maneuvers. The colored background contains the identified regions where quasi-constant velocity models are valid based on the PM task.

Similar to results in the static pedestrian avoidance case, anomaly measurements generated by models trained with the PM task applied to the scenario III are shown in Fig. 16. Three patterns can be distinguished in such image; they are “stop maneuver”, “curve execution” and “straight path”. It is possible to see an abnormality pattern (notice the blue ovals in Fig. 16) consisting of a prominent peak that periodically shows up. Such peaks represent the emergency stop maneuver.

As explained previously in the avoidance case, subtle differences between curves performances produce some deviations from normality. Nonetheless, only a few curving points present abnormalities. Moreover, their level anomaly is low in comparison to the stop maneuver.

Fig. 17b shows the observations from scenario III where high abnormalities take place. Such measurements can be used potentially for creating new models into the set of KFs.

## VII. CONCLUSION AND FUTURE WORK

This paper presents a method for detecting abnormalities in observed trajectories by using a set of KFs built incrementally as new experiences occur. Such bank of filters is created based on a non-motivated dynamical model from which more complex dynamics are approximated and added into the available inference models.

A decomposition of GP regression based on a superpixel-like approach is applied to obtain zones where quasi-constant velocity models are valid. Generated zones are employed for prediction and abnormality detection in real data from a vehicle performing a series of tasks in a controlled scene.

A strategy for detecting abnormalities based on innovation measurements is tested by using real vehicle's trajectories. The proposed method analyzes motion maneuvers containing information concerning an interplay between vehicle and pedestrians. Results suggest that our methodology facilitates to find abnormalities in an online way and identify anomaly observations (unknown maneuvers) that can be potentially learned as new models to be integrated into the set of KFs.

Since abnormalities in vehicle-pedestrian interaction cases can be automatically recognized and characterized, the present work can be used in the future for understanding more complex traffic scenarios by autonomous vehicles. Accordingly, forthcoming works include developments towards optimizing intelligent transportation decision making by encoding situations semantically into expert systems. From that viewpoint, this work can be employed in future research for increasing the awareness of smart mobility systems by understanding the vehicles' dynamics through the observation of their locations in time. Future developments of the presented methodology will converge to the next generation of autonomous vehicles providing a safe and reliable automatic driving.

## REFERENCES

- [1] J. Nilsson, M. Bränström, E. Coelingh, and J. Fredriksson, "Lane change maneuvers for automated vehicles," *IEEE Trans. Intell. Transp. Syst.*, vol. 18, no. 5, pp. 1087–1096, May 2017.
- [2] D. González, J. Pérez, V. Milanés, and F. Nashashibi, "A review of motion planning techniques for automated vehicles," *IEEE Trans. Intell. Transp. Syst.*, vol. 17, no. 4, pp. 1135–1145, Apr. 2016.
- [3] S. Chawla, Y. Zheng, and J. Hu, "Inferring the root cause in road traffic anomalies," in *Proc. IEEE 12th Int. Conf. Data Mining (ICDM)*, Dec. 2012, pp. 141–150.
- [4] B. Mathibela, P. Newman, and I. Posner, "Reading the road: Road marking classification and interpretation," *IEEE Trans. Intell. Transp. Syst.*, vol. 16, no. 4, pp. 2072–2081, Aug. 2015.
- [5] E. Galceran and M. Carreras, "A survey on coverage path planning for robotics," *Robot. Auton. Syst.*, vol. 61, no. 12, pp. 1258–1276, 2013.
- [6] M. Elhoussi, J. Georgy, A. Noureddin, and M. J. Korenberg, "A survey on approaches of motion mode recognition using sensors," *IEEE Trans. Intell. Transp. Syst.*, vol. 18, no. 7, pp. 1662–1686, Jul. 2017.
- [7] B. Krausz and C. Bauckhage, "Analyzing pedestrian behavior in crowds for automatic detection of congestions," in *Proc. IEEE Int. Conf. Comput. Vis. Workshops*, Nov. 2011, pp. 144–149.
- [8] Y. Zheng, L. Capra, O. Wolfson, and H. Yang, "Urban computing: Concepts, methodologies, and applications," *ACM Trans. Intell. Syst. Technol.*, vol. 5, no. 3, p. 38, 2014.
- [9] R. Yu, Y. Zhang, S. Gjessing, W. Xia, and K. Yang, "Toward cloud-based vehicular networks with efficient resource management," *IEEE Netw.*, vol. 27, no. 5, pp. 48–55, Sep./Oct. 2013.
- [10] Q. Hu and L. Xu, "Real-time road traffic awareness model based on optimal multi-channel self-organized time division multiple access algorithm," *Comput. Elect. Eng.*, vol. 58, pp. 299–309, Feb. 2017.
- [11] S. Djahel, R. Doolan, G.-M. Muntean, and J. Murphy, "A communications-oriented perspective on traffic management systems for smart cities: Challenges and innovative approaches," *IEEE Commun. Surveys Tuts.*, vol. 17, no. 1, pp. 125–151, Mar. 2015.
- [12] Y. Zheng, Y. Liu, J. Yuan, and X. Xie, "Urban computing with taxicabs," in *Proc. 13th Int. Conf. Ubiquitous Comput.*, Sep. 2011, pp. 89–98.
- [13] A. Awasthi, K. Venkitusamy, S. Padmanaban, R. Selvamuthukumaran, F. Blaabjerg, and A. K. Singh, "Optimal planning of electric vehicle charging station at the distribution system using hybrid optimization algorithm," *Energy*, vol. 133, pp. 70–78, Aug. 2017.
- [14] W. Min and L. Wynter, "Real-time road traffic prediction with spatio-temporal correlations," *Transp. Res. C Emerg. Technol.*, vol. 19, no. 4, pp. 606–616, 2011.
- [15] L.-Y. Wei, Y. Zheng, and W.-C. Peng, "Constructing popular routes from uncertain trajectories," in *Proc. 18th SIGKDD Conf. Knowl. Discovery Data Mining*, Aug. 2012, pp. 1–9.
- [16] A. Fernández-Ares *et al.*, "Studying real traffic and mobility scenarios for a Smart City using a new monitoring and tracking system," *Future Gener. Comput. Syst.*, vol. 76, pp. 163–179, Nov. 2017.
- [17] M. Castro-Neto, Y.-S. Jeong, M.-K. Jeong, and L. D. Han, "Online-SVR for short-term traffic flow prediction under typical and atypical traffic conditions," *Expert Syst. Appl.*, vol. 36, no. 3, pp. 6164–6173, 2009.
- [18] K. Zheng, Y. Zheng, N. J. Yuan, and S. Shang, "On discovery of gathering patterns from trajectories," in *Proc. IEEE 29th Int. Conf. Data Eng.*, Apr. 2013, pp. 242–253.
- [19] D. Campo, M. Baydoun, L. Marcenaro, and A. Cavallaro, "Modeling and classification of trajectories based on a Gaussian process decomposition into discrete components," in *Proc. 14th IEEE Int. Conf. Advance Video Signal Based Survill.*, Aug. 2017, pp. 1–6.
- [20] C. Guo, K. Kidono, and M. Ogawa, "Learning-based trajectory generation for intelligent vehicles in urban environment," in *Proc. IEEE Intell. Vehicles Symp. (IV)*, Jun. 2016, pp. 1236–1241.
- [21] S. Chen, C. Claramunt, and C. Ray, "A spatio-temporal modelling approach for the study of the connectivity and accessibility of the Guangzhou metropolitan network," *J. Transp. Geography*, vol. 36, pp. 12–23, Apr. 2014.
- [22] L. Tong, X. Zhou, and H. J. Miller, "Transportation network design for maximizing space-time accessibility," *Transp. Res. B, Methodol.*, vol. 81, pp. 555–576, Nov. 2015.
- [23] G. Piriou, P. Bouthemy, and J. F. Yao, "Recognition of dynamic video contents with global probabilistic models of visual motion," *IEEE Trans. Image Process.*, vol. 15, no. 11, pp. 3417–3430, Nov. 2006.
- [24] D. Campo, V. Bastani, L. Marcenaro, and C. Regazzoni, "Incremental learning of environment interactive structures from trajectories of individuals," in *Proc. 19th Int. Conf. Inf. Fusion*, Jul. 2016, pp. 589–596.
- [25] B. T. Morris and M. M. Trivedi, "A survey of vision-based trajectory learning and analysis for surveillance," *IEEE Trans. Circuits Syst. Video Technol.*, vol. 18, no. 8, pp. 1114–1127, Aug. 2008.
- [26] D. Campo, A. Betancourt, L. Marcenaro, and C. Regazzoni, "Static force field representation of environments based on agents' nonlinear motions," *EURASIP J. Adv. Signal Process.*, vol. 2017, no. 1, p. 13, Dec. 2017.
- [27] V. Bastani, L. Marcenaro, and C. S. Regazzoni, "Online nonparametric Bayesian activity mining and analysis from surveillance video," *IEEE Trans. Image Process.*, vol. 25, no. 5, pp. 2089–2102, May 2016.
- [28] S. Zhou, Z. Zhang, D. Zeng, and W. Shen, "Abnormal events detection in crowded scenes by trajectory cluster," in *Proc. 9th Int. Symp. Precis. Eng. Meas. Instrum.*, vol. 9446, Mar. 2015, Art. no. 944614.
- [29] M. Y. Choong, L. Angeline, R. K. Y. Chin, K. B. Yeo, and K. T. K. Teo, "Vehicle trajectory clustering for traffic intersection surveillance," in *Proc. IEEE Int. Conf. Consum. Electron.-Asia*, Oct. 2016, pp. 1–4.
- [30] P. Crook and G. Hayes, "A robot implementation of a biologically inspired method for novelty detection," in *Proc. Towards Intell. Mobile Robots Conf.*, Apr. 2001, pp. 1–10.
- [31] F. Castaldo, F. A. N. Palmieri, V. Bastani, L. Marcenaro, and C. Regazzoni, "Abnormal vessel behavior detection in port areas based on dynamic Bayesian networks," in *Proc. 17th Int. Conf. Inf. Fusion (FUSION)*, Jul. 2014, pp. 1–7.
- [32] K. Kim, D. Lee, and I. Essa, "Gaussian process regression flow for analysis of motion trajectories," in *Proc. IEEE Int. Conf. Comput. Vis.*, Nov. 2011, pp. 1164–1171.
- [33] J. Wang, J. Wu, and Y. Li, "The driving safety field based on driver-vehicle-road interactions," *IEEE Trans. Intell. Transp. Syst.*, vol. 16, no. 4, pp. 2203–2214, Aug. 2015.
- [34] J. Choi *et al.*, "Environment-detection-and-mapping algorithm for autonomous driving in rural or off-road environment," *IEEE Trans. Intell. Transp. Syst.*, vol. 13, no. 2, pp. 974–982, Jun. 2012.
- [35] M. Czubenko, Z. Kowalcuk, and A. Ordys, "Autonomous driver based on an intelligent system of decision-making," *Cogn. Comput.*, vol. 7, no. 5, pp. 569–581, Oct. 2015.
- [36] Y. Yusof, H. A. H. Mansor, and A. Ahmad, "Formulation of a lightweight hybrid AI algorithm towards self-learning autonomous systems," in *Proc. IEEE Conf. Syst., Process Control (ICSPC)*, Dec. 2016, pp. 142–147.

- [37] X. Zhang, X. Ruan, Y. Xiao, and J. Huang, "Sensorimotor self-learning model based on operant conditioning for two-wheeled robot," *J. Shanghai Jiaotong Univ. Sci.*, vol. 22, no. 2, pp. 148–155, Apr. 2017.
- [38] H. Jeong, H. J. Chang, and J. Y. Choi, "Modeling of moving object trajectory by spatio-temporal learning for abnormal behavior detection," in *Proc. IEEE Int. Conf. Adv. Video Signal Based Surveill.*, Aug. 2011, pp. 119–123.
- [39] C. Li, Z. Han, Q. Ye, and J. Jiao, "Abnormal behavior detection via sparse reconstruction analysis of trajectory," in *Proc. 6th Int. Conf. Image Graph.*, Aug. 2011, pp. 807–810.
- [40] X. Wang, K. Tieu, and E. Grimson, *Learning Semantic Scene Models by Trajectory Analysis*. Berlin, Germany: Springer, 2006, pp. 110–123.
- [41] Z. Li and J. Chen, "Superpixel segmentation using linear spectral clustering," in *Proc. IEEE Conf. Comput. Vis. Pattern Recognit.*, Jun. 2015, pp. 1356–1363.
- [42] X. Wang, X. Ma, and W. E. L. Grimson, "Unsupervised activity perception in crowded and complicated scenes using hierarchical Bayesian models," *IEEE Trans. Pattern Anal. Mach. Intell.*, vol. 31, no. 3, pp. 539–555, Mar. 2009.
- [43] C. E. Rasmussen. (2016). *Documentation for GPML MATLAB Code Version 4.0*. [Online]. Available: <http://www.gaussianprocess.org/gpml/code/matlab/doc/>
- [44] D. Helbing and P. Molnar, "Social force model for pedestrian dynamics," *Phys. Rev. E, Stat. Phys. Plasmas Fluids Relat. Interdiscip. Top.*, vol. 51, no. 5, pp. 4282–4286, 1995.
- [45] P. Marín *et al.*, "Stereo vision-based local occupancy grid map for autonomous navigation in ROS," in *Proc. Int. Conf. Comput. Vis., Imag. Comput. Graph. Theory Appl.*, Mar. 2016, pp. 1–6.
- [46] M. Quigley *et al.*, "ROS: An open-source robot operating system," in *Proc. ICRA Workshop Open Sour. Softw.*, 2009, vol. 3, no. 3.2, p. 5.
- [47] J. Zhang and S. Singh, "LOAM: Lidar odometry and mapping in real-time," *Robotics, Sci. Syst.*, vol. 2, p. 9, Jul. 2014.



**Damian Campo** received the degree in engineering physics from EAFIT University, Medellin, Colombia, in 2014, and the Ph.D. degree in cognitive environments from the University of Genoa, Italy, in 2018. His research interests include the application of machine learning techniques for modeling dynamics of cognitive entities and predict future states of dynamical systems by using probabilistic theory.



**Mohamad Baydoun** received the bachelor's degree in telecommunication engineering and the M.S. degree in telecommunication systems engineering from the University of Genoa, Italy, in 2011 and 2015, respectively. He is currently pursuing the Ph.D. degree in interactive and cognitive environments with the University of Genoa. His interests are machine learning and signal processing applications for abnormality detection purposes.



**Pablo Marin** received the degree in Industrial engineering in 2011. The same year, he obtained the degree in Electronics and Automation engineering from the same University. In 2013, he received his Master degree in Robotics and Automation. He completed his Ph.D. under the Advanced Driver Assistance Systems (ADAS) project in 2019. All his degrees have been conferred by the University Carlos III. His current research interests include computer vision and autonomous ground vehicle.



**David Martin** received the degree in industrial physics (automation) from the National University of Distance Education (UNED) in 2002 and the Ph.D. degree in computer science from the Spanish Council for Scientific Research (CSIC) and UNED, Spain, in 2008. Since 2011, he has been a member of the Intelligent Systems Lab. He is currently a Professor and a Post-Doctoral Researcher with the Carlos III University of Madrid. He was a recipient of the VII Barreiros Foundation Award for the best research in the automotive field in 2014. In 2015, he has awarded as the Best Reviewer of the 18th IEEE International Conference on Intelligent Transportation Systems by the IEEE Society.



**Lucio Marcenaro** received the degree in electronic engineering and the Ph.D. degree in computer science and electronic engineering from Genoa University in 1999 and 2003, respectively. Since 2011, he has been an Assistant Professor of telecommunications with the Faculty of Engineering, Department of Electrical, Electronic, Telecommunications Engineering and Naval Architecture (DITEN), University of Genoa. He has over 15 years of experience in image and video sequence analysis. He has authored about 100 technical papers related to signal and video processing for computer vision.



**Arturo de la Escalera** received the degree in automation and electronics engineering and the Ph.D. degree in robotics from the Universidad Politécnica de Madrid, Madrid, Spain, in 1989 and 1995, respectively. In 1993, he joined the Department of Systems Engineering and Automation, Universidad Carlos III de Madrid, Madrid, where he became an Associate Professor in 1997. Since 2005, he has been the Head of the Intelligent Systems Lab (LSI). Since 2012, he has been an Assistant Director of the Engineering School, Universidad Carlos III de Madrid. He is an Editorial Board Member of the *International Journal of Advanced Robotic Systems: Robot Sensors* (Intech), the *International Journal of Information and Communication Technology* (InderScience Publisher), the *Open Transportation Journal* (Bentham Science Publishers), the *Scientific World Journal: Computer Science* (Hindawi Publishing Corporation), and the *Revista Iberoamericana de Automática e Informática Industrial*.



**Carlo Regazzoni** is currently a Full Professor of cognitive telecommunications systems with DITEN, University of Genoa, Italy. He has been responsible for several national and EU funded research projects. He is a Coordinator of international Ph.D. courses on interactive and cognitive environments involving several European universities. He served as the General Chair for several conferences and an Associate Editor/Guest Editor for several international technical journals. He has served in many roles for governance bodies of the IEEE SPS. He served as a Vice President Conferences for the IEEE Signal Processing Society from 2015 to 2017.